Radiation-induced degradation of doxazosin: Role of reactive species, toxicity, mineralization and degradation pathways

Ivana Tartaro Bujak[1*], Marijana Pocrnić[2], Karlo Blažek[1], Krunoslav Bojanić[3,4], Polonca Trebše[5], Albert T. Lebedev[6], Nives Galić[2]

[1]Radiation Chemistry and Dosimetry Laboratory, Ruđer Bošković Institute, Bijenička c. 54, 10 000 Zagreb, Croatia

[2]Department of Chemistry, Faculty of Science, University of Zagreb, Horvatovac 102a, 10 000 Zagreb, Croatia

[3]Laboratory for Aquaculture Biotechnology, Division of Materials Chemistry, Ruđer Bošković Institute, Bijenička c. 54, 10 000 Zagreb, Croatia

[4]Centre of Excellence for Marine Bioprospecting-BioProCro, Ruđer Bošković Institute, Zagreb, Croatia

[5]University of Ljubljana, Faculty of Health Sciences, Ljubljana, Slovenia

[6]Masseco, d.o.o., Postojna, Slovenia

*Corresponding author: Ivana Tartaro Bujak, e-mail: itartaro@irb.hr

Abstract

State-of-the-art technologies based on advanced oxidation processes (AOPs) are currently being developed for the removal of environmental pollutants such as pharmaceuticals from water matrices. Such studies are very important and should include the impact of inorganic and organic matrix on the degradation process of pollutants. One of the AOPs that is in focus of investigations nowadays, is ionizing radiation. Doxazosin (DOX) is a widely used pharmaceutical for the treatment of hypertension, which can be potentially harmful due to its occurrence in the aquatic environment. This study reports the radiation-induced degradation of DOX in aqueous solution. Removal of 10 mg L^{-1} DOX reached almost 100 % at irradiation doses of 200 Gy regardless of the dose rate used. The effect of saturated solutions with N_2, N_2O, air and the addition of radical scavengers such as 2-PrOH and thiourea on DOX degradation was investigated. The efficiency of degradation increased in the order: thiourea < 2-PrOH < N_2 < air < N_2O. The effects of pH, various inorganic ions and water matrix on DOX degradation were also studied. DOX degradation was lower in underground water than in ultrapure water. Under prolonged irradiation, mineralization of about 60 % of DOX solutions was observed based on the dissolved organic carbon (DOC) evaluation. Toxicity tests with *V. fischeri* luminescent bacteria showed higher toxicity of samples irradiated at 500 Gy. The main degradation products were identified using LC-HRMS and degradation pathways were proposed. Overall, irradiation technology could be a promising technique for the removal of micropollutants, such as pharmaceuticals in real water matrices.

Keywords: doxazosin, degradation, ionizing radiation, LC-MS, toxicity

1. Introduction

Water resources and water quality have been a major environmental concern in recent decades due to rapid population growth, aging population, and current climate change. Due to the growing demand for pharmaceuticals, their presence in the environment is also increasing. Several studies have reported the presence of environmental pollutants, including pharmaceuticals in water, indicating that conventional wastewater techniques such as membrane filtration, activated carbon adsorption, reverse osmosis, etc., are unable to efficiently remove emerging pollutants from effluents [1-10]. The concentrations of pharmaceuticals detected in wastewater can vary from ng L^{-1} to μg L^{-1} and in surface waters up to ng L^{-1} [11, 12]. However, it was shown that even extremely low concentrations may have harmful effect on living organisms [13, 14, 15]. Therefore, it is critical to find a technique that can effectively remove pharmaceuticals from water. Each treatment has advantages and constraints. Nevertheless, adsorption is often cited as the process of choice for the removal of many different types of pollutants because it is simple in design, easy to apply, inexpensive and efficient. However, the main disadvantage is the weak selectivity and the adsorbent used requires further treatment for complete removal of the pollutants and regeneration of the adsorbent. On the other hand, ionizing radiation treatment is a novel process among Advanced Oxidation Processe (AOP). It is a promising, unique and environmentally friendly technique for the effective removal of pharmaceuticals by their decomposition. The advantages of gamma irradiation over other AOPs include good penetration into the water matrix, high efficacy, no need for chemicals, and no secondary contamination [16]. This method has been widely studied and found to be more efficient and cost-effective than other AOPs [17, 18, 19]. In addition, the usefulness and efficiency of radiation technology for treating various organic pollutants have been sufficiently demonstrated at different scales. Recently, great progress has been made in wastewater treatment by applying radiation technology on an industrial scale [20, 21].

The application of ionizing radiation for pollutants degradation in water is based on simultaneous generation of reactive oxidizing and reducing species during the radiolysis of water, which can then directly react with pollutants. Gamma irradiation of an aqueous solution produces highly reactive radicals, mainly $HO^{\bullet}$, $H^{\bullet}$ and e^{-}_{aq} along with some molecular products and ions. The extent of their production depends on several factors: the pH of the solution, the temperature, the energy emitted per unit distance by the incident radiation in the aqueous medium, the absorbed dose, the dose rate, and the presence of dissolved gases. In some cases oxidation by $^{\bullet}OH$ radicals is slow and the application of reducing radicals, such as $H^{\bullet}$ and $e^{-}_{aq,}$ may be useful.

In natural waters and wastewaters, organic matter and various inorganic salts such as chlorides, nitrates, nitrites, carbonates, bicarbonates and sulfates have also important influence on the performance of AOPs. Many studies on AOPs applications [22, 23, 24, 25, 26, 27, 28, 6] showed that the effect of inorganic anions on the degradation process of pollutants varies depending on the concentration and type of inorganic anions. Comparing some of the most common anions, the nitrite ion (NO_2^-) is the most efficient $^{\bullet}OH$ scavenger. Other efficient scavengers are NO_3^-, CO_3^{2-}, HPO_4^{2-} and HCO_3^- [23, 24, 25].

Among widely used pharmaceuticals, antihyperthesive drugs are well-known pollutants. Doxazosin (DOX), 1-[(4-amino-6,7-dimethoxy-2-quinazolinyl)-4-(1,4-benzodioxan-2-yl-carbonyl)-piperazine monomethanesulfonate], is a drug used preferentially to treat hypertension and benign prostatic hyperplasia, and very low concentrations of DOX have been detected in raw water [4]. In our previous publication [29], photolytic and photocatalytic degradation of DOX with TiO_2 were studied. It was found that DOX degradation was more effective in photocatalytic degradation with TiO_2/ UVA than photolysis, but inefficient in complete mineralization. In the present study, we extended the research by using another AOP technique, the gamma irradiation technique, for the degradation of DOX in an

aqueous solution since the effects of gamma irradiation on the degradation of DOX have not been studied yet. The factors affecting DOX degradation, such as dose rate, the influence of inorganic ions, water matrix, and pH, were investigated. UV-Vis spectroscopy, HPLC-DAD and LC-HR MS/MS were used to detect and identify the degradation products, and possible degradation pathways were proposed. Mineralization of DOX during gamma irradiation and its toxicity were examined as well.

2. Materials and methods

2.1. Materials

Doxazosin mesylate (DOX), analytical standard, was provided by Sigma-Aldrich (≥ 97 %, HPLC). The chemical structure and characteristics of DOX are displayed in Table 1. Chemicals for HPLC-DAD analyses were as follows: glacial acetic acid 100 % p.a. from Merck, ammonium acetate from Gram-mol, acetonitrile from Honeywell (HPLC). Potassium hydrogen phosphate and sodium hydroxide were purchased from Kemika. Methanol and 2-propanol were purchased from Honeywell (HPLC grade). Sodium nitrate was obtained from Lach-Ner, sodium hydrogen carbonate from Gram-Mol and thiourea was purchased from Sigma. Formic acid and acetonitrile for LC-MS analysis were purchased from Carlo Erba (MS grade). Ultrapure water was obtained from the Mili-Q Advantage A10 purification system (Merck). All chemicals were used as received without any further purification.

Table 1. Chemical and physical properties of doxazosin (1-[(4-amino-6,7-dimethoxy-2-quinazolinyl)-4-(1,4-benzodioxan-2-yl-carbonyl)-piperazine monomethanesulfonate]).

Molecular formula	$C_{24}H_{29}N_5O_8S$
Chemical structure	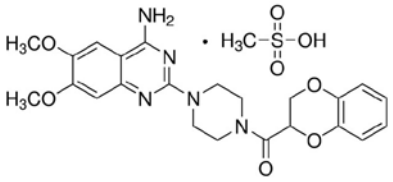
Molecular weight (g/mol)	547.6
Solubility	Freely soluble in dimethylsulfoxide Slightly soluble in methanol, ethanol and water (0.8 % at 25 °C)
pK_a	5.45
Boiling temperature	275-277 °C
Melting temperature	718 °C

2.2. Irradiation studies

Aqueous solutions of DOX were prepared daily in concentrations 1.9×10^{-5} mol L^{-1}. The experiments were carried out in ultrapure water to allow the identification of products formed exclusively from the degradation of DOX and not from the reactions of DOX with other substances present in the environment. The pH of the unbuffered solutions was 6.6. The samples for the end-product experiments were irradiated in a panoramic type ^{60}Co-γ irradiation chamber with different dose rates and with the following doses: 0, 0.2, 0.4, 0.6, 0.8, 1 and 2 kGy. Dose mapping of the irradiation facility has been performed experimentally (using ionizing chambers and ECB dosimetric system) and by simulation calculations [30]. Test solutions were in equilibrium with air or saturated with N_2 or N_2O in 15 cm^3 ampoules (and thereafter airtight sealed) prior to irradiation investigation. When the hydrated electron

reactions were studied 2-propanol (2-PrOH) (0.2 mmol L^{-1}) was applied to scavenge the hydroxyl radicals. The temperature was kept constant during the irradiation process at 20 ± 2 °C.

To investigate the effect of inorganic anions on the degradation of DOX, an aliquot of the stock solution was added prior to irradiation. The final concentration of $NaHCO_3$ was 1.9 mmol L^{-1}, $NaNO_3$ 1 mmol L^{-1} and K_2HPO_4 was 7 mg L^{-1}, respectively. All solutions were purged with N_2.

The matrix effect was studied using groundwater instead of ultrapure water.

2.2.1 Calculation of G-value

The G-value is defined as the number of molecules in μmol, produced or decomposed when absorbing 1 J of energy. It was calculated using the following equation (Spinks and Woods, 1990):

$$G = \frac{[R]}{D} \times 10^6 \quad (1)$$

R is the disappearance in the reactant concentration, DOX (mol L^{-1}), *D* the absorbed dose (Gy).

2.3. Analytical procedures

2.3.1. HPLC-DAD measurements and UV-Vis spectrometry

Aqueous solutions of DOX were analyzed by HPLC-DAD (UV-Vis) KNAUER K-501 (Germany). The separation was achieved using Nucleosil C18 column (5 μm, 4.0 × 250 mm). The column thermostat was maintained at 25 °C and the injection volume was 100 μL. The mobile phase consisted of acetonitrile (A) and ammonium acetate (2.5 mM, pH 4) (B). The ratio of eluent A and eluent B was changed from initial 60 / 40 to 30 / 70 over 15 minutes. The

157 flow rate was 1.5 mL min^{-1} and the monitored wavelengths were 247 nm and 330 nm. The
158 retention time for DOX was 7.1 min.
159 The absorption spectra of DOX within irradiation time were recorded in the wavelength
160 range of 200-800 nm using UV-Vis spectrophotometer, Varian Cary 4000.
161
162 ***2.3.2. Identification of products by LC-HRMS/MS***
163 Degradation products were analyzed by high pressure liquid chromatography - high-resolution
164 mass spectrometry using Agilent 6550 Series Accurate-Mass-Quadrupole Time-of-Flight mass
165 spectrometer coupled with Agilent 1290 Infinity II UHPLC. Samples for tandem mass
166 spectrometry (LC-HRMS/MS) analysis have been concentrated 10 times in order to detect
167 maximal number of reaction products. Chromatographic separation was performed on Zorbax
168 Eclipse Plus C18 (1.8 μm, 2.1 × 50 mm) column. The mobile phase consisted of 0.1 % formic
169 acid in water (A) and acetonitrile (B). Elution was performed by gradient profile as follows: 0
170 min 90 % A; 10 min 50 % A; 12 min 30 % A. Flow rate was set at 0.4 mL min^{-1}, column
171 temperature was 30 °C and the injection volume was 5 μL. The electrospray ionization was
172 performed in positive mode in the mass range 100 – 800 *m/z* for MS analysis and 50 – 500 *m/z*
173 for MS/MS analysis. Collision-induced dissociation was performed using collision energies
174 (CE) 10 V, 20 V and 40 V. The other parameters of mass spectrometer were optimized as
175 follows: capillary voltage, 3500 V; sheath gas temperature, 350 °C; sheath gas flow rate, 11 L
176 min^{-1}; drying gas temperature, 200 °C; and drying gas flow rate, 14 L min^{-1}. Nitrogen was used
177 as drying and sheath gas.
178
179 ***2.3.3.Dissolved organic carbon (DOC) measurements***
180 DOC concentrations were determined using the sensitive High-Temperature Catalytic
181 Oxidation (HTCO) method at 680 °C (Shimadzu total organic carbon analyzer model TOC-

Vcph with Pt/Si catalyst, calibrated with potassium hydrogen phthalate). Non-Dispersive Infrared (NDIR) detector for CO_2 was used for DOC measurements. Pt on silica was used as a catalyst to determine the dissolved fraction (DOC). Samples were acidified to pH 2 with 2 mmol L^{-1} HCl and purged with pure air for 10 min prior to analysis in order to eliminate the inorganic carbon. The concentration was calculated as an average of three to five replicates [31].

2.3.4. Toxicity experiments (Antimicrobial activity)

Untreated sampes and samples treated with 50, 100 and 500 Gy were tested for antimicrobial activity against *Staphylococcus aureus* ATCC 6538 and an environmental isolate of *Vibrio fischeri* from the Adriatic Sea using a broth microdilution method according to the CLSI guidelines [32] with minor modifications. Bacterial strains were recovered from –80 °C using tryptone soya agar (Biolab, Hungary). Fresh overnight growth was used to prepare inocula to 0.5 McFarland by turbidity adjustment in 5 mL of sterile phosphate-buffered solution using a turbidimeter (bioMérieux, France) and thereafter diluted with cation-adjusted Mueller-Hinton broth (Merck, Germany) to reach the final concentration of ~5×10^5 CFU mL^{-1} per well. All assays employed positive (inoculated media without the tested sample) and negative (sterile media) control. All cultivations of bacteria and assays were performed aerobically at 30 ºC and in duplicates. The concentration range tested was from 2.5 ppm to 0.005 ppm. Briefly, sample solutions of 10 ppm were 2-fold diluted with culture broth and 100 µL placed in first column of microtitre plates. Columns 2 to 10 were filled with 50 µL of culture broth and serial 2-fold dilutions of test samples were performed by transferring 50 µL using multichannel pipette and discarded after the 10th column as columns 11 and 12 were reserved for positive and negative controls, respectively. Thereafter, the wells were filled with 50 µL of culture broth diluted bacterial inocula (except column 12) to obtain final bacterial concentration of ~5×10^5 CFU

mL^{-1} in a total reaction volume of 100 µL. Results were interpreted both visually and spectrophotometrically using a microplate reader (Tecan, Austria). Plates were first shaken for 10 s in orbital mode with an amplitude of 3 mm and then absorbance was scanned at wavelength of 600 nm (OD600) with 25 flashes after 100 ms of settle time with microtitre lid in place. Since no complete inhibition of bacterial growth was observed, the growth in each well was expressed as a percentage relative to the growth in respective positive control wells.

2.3.5. Statistical analysis

All experimental results were performed at least in triplicate ($n \geq 3$) in order to evaluate the reproducibility of measurements the data are expressed as means ± SD.

3. Results and discussion

The degradation of DOX in aqueous solution by gamma irradiation was investigated under different experimental conditions (dose rate, pH, presence of inorganic salts, presence of dissolved gases) since the production of reactive radicals like $^{\bullet}OH$, $H^{\bullet}$ and e^{-}_{aq} depends on those factors. In addition to the generation of strong oxidants $^{\bullet}OH$ by gamma radiation, the radiolysis of water generates the same amount of reducing species (Eq. 2):

$$H_2O \xrightarrow{\sim\sim} (0.28)\ e_{aq}^{-},\ (0.062)\ H^{\bullet},\ (0.28)\ ^{\bullet}OH,\ (0.047)\ H_2,\ (0.073)\ H_2O_2,\ (0.28)\ H_3O^{+} \quad (2)$$

The values in the brackets represent the *G*-values of each species in units of μmol J^{-1}.

3.1. The dose rate influence

A typical decomposition curve of DOX by γ-radiation at different dose rates is shown in Fig. 1.

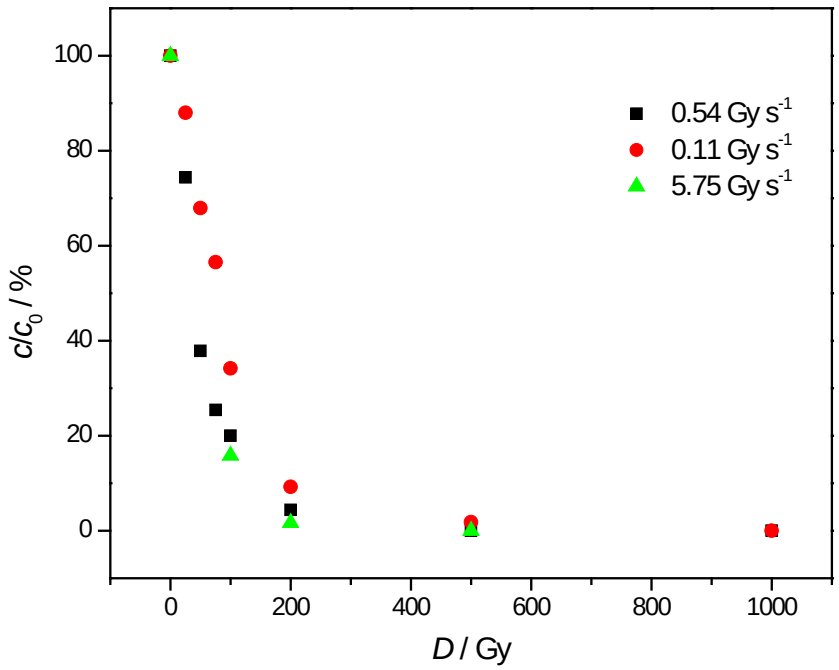

Figure 1. The effect of dose rate on degradation of DOX under aerobic conditions.

Experiments were performed in duplicate to ensure the reproducibility of data for each irradiation dose. At an absorbed dose of 200 Gy, the degradation of DOX increased from 90.7 to 95.6 and 98.3 % with increasing dose rate from 0.11, to 0.54 and 5.75 Gy s^{-1}, respectively. At a higher dose rate, the amount of energy absorbed by water molecules increases, leading to a higher concentration of primary radicals and thus to a higher DOX degradation rate. The decomposition of DOX by γ-irradiation was compared with the calculated *G*-values (Eq. 1). At an initial DOX concentration of 10 mg L^{-1}, the *G*-values decreased with the increase of the absorbed dose from 100 Gy to 1000 Gy (Table 2), which was also reported in several other studies [16, 18, 33].

Table 2. *G*-values of DOX in aqueous solution irradiated under air, γ(DOX) = 10 mg L^{-1}

Absorbed dose / Gy	*G*-value / μmol J^{-1}		
	5.75 Gy s^{-1}	0.54 Gy s^{-1}	0.11 Gy s^{-1}
50	/	0.236	0.122
100	0.161	0.151	0.125
200	0.090	0.09	0.086
500	0	0	0.037
1000	0	0	0

The decreasing trend of *G*-values could be due to the increased possibility of radicals recombination reactions (Eq. 3-6) (Buxton et al., 1988, 33) competing with radical-pollutant reactions. Basfar and co-authors [33] also suggested that at higher radiation doses, the by-products formed could compete with the parent compound for the radicals.

$$^{\bullet}OH + {}^{\bullet}H \longrightarrow H_2O \qquad (k = 7 \times 10^9\ M^{-1}\ s^{-1}) \qquad (3)$$

$$^{\bullet}OH + {}^{\bullet}OH \longrightarrow H_2O_2 \qquad (k = 5.5 \times 10^9\ M^{-1}\ s^{-1}) \qquad (4)$$

$$^{\bullet}OH + e_{aq}^{-} + {}^{\bullet}H \longrightarrow H_2 + OH^{-} \qquad (k = 2.5 \times 10^{10}\ M^{-1}\ s^{-1}) \qquad (5)$$

265 $^{\bullet}OH + e_{aq}^{-} \longrightarrow OH^{-}$ ($k = 3.0 \times 10^{10}\ M^{-1}\ s^{-1}$) (6)

266 ***3.2. Radicals involved in decomposition of DOX (P = 0.54 Gy s^{-1})***

267 To investigate the effect of different reactive species on the radiolytic decomposition of DOX,
268 radical scavengers were used before irradiation: air, N_2O, N_2, 2-PrOH and thiourea. The
269 optimal dose rate of 0.54 Gy s^{-1} was used. The UV-Vis spectra of DOX after the irradiation
270 under different conditions are shown in Fig. 2. Since thiourea absorbes in the same UV-Vis
271 region as DOX, the influence of radicals involved in decomposition was monitored by HPLC.
272 It is clear that DOX was degraded under all experimental conditions, and the degradation was
273 increased with an increase in irradiation dose.

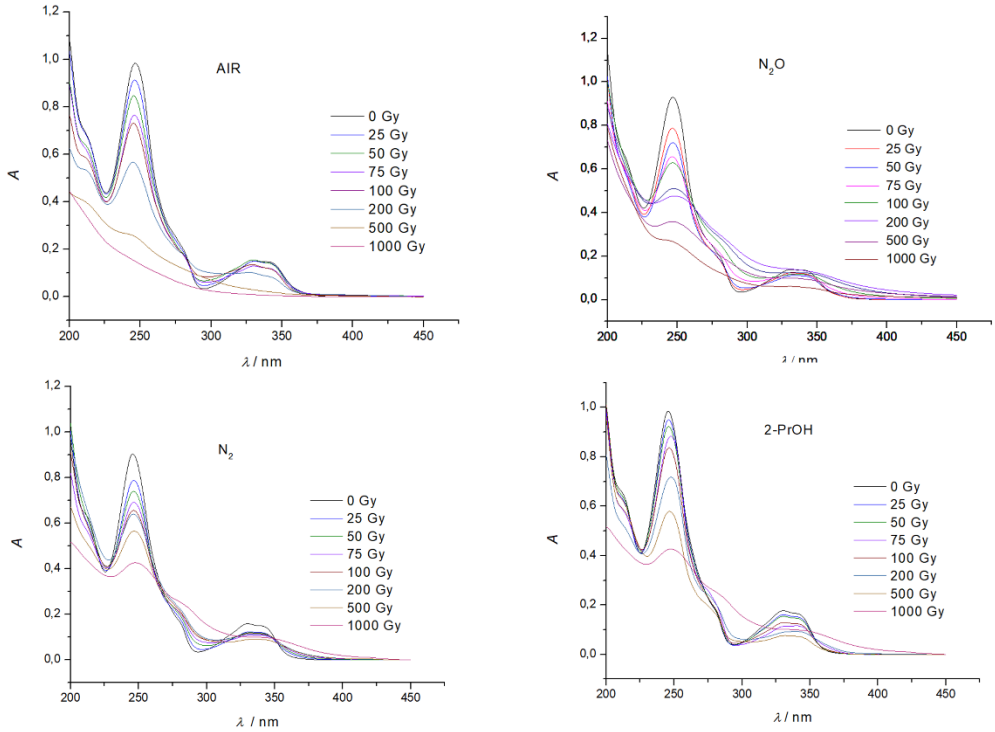

274

275

276 Figure 2. UV-Vis spectra of DOX degradation under different conditions.

277 As shown in Fig. 3., the degradation of DOX at 100 Gy was almost complete under N_2O
278 conditions, 80 % of DOX was degraded in equilibrium with air, 73.4 % was degraded under
279 N_2 conditions, 32.2 % was degraded by the addition of 2-PrOH and only 7 % was degraded in
280 the presence of thiourea. The efficiency of degradation increased in the following order:
281 thiourea < 2-PrOH < N_2 < air < N_2O. The explanation for this behaviour may become clearer
282 if one looks at the individual reactions under different experimental conditions.

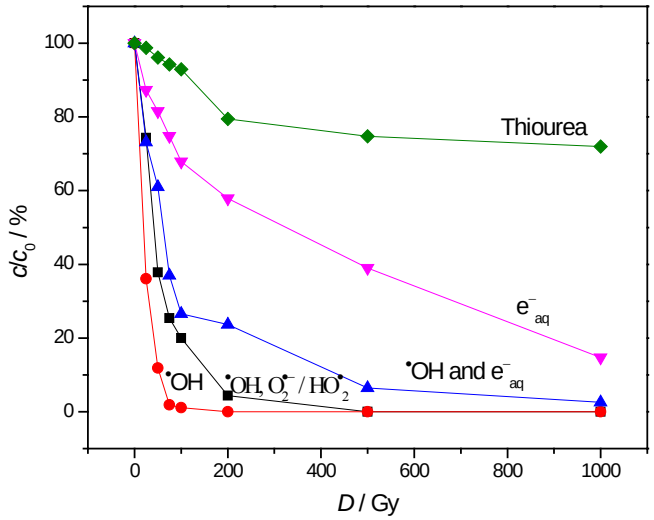

Figure 3. The influence of radicals involved in the decomposition of DOX.
N_2O (●), air (■), N_2 (▲), 2-PrOH (▼), thiourea (♦)

In experiments performed in aerated conditions the reactions presented in equations 7-9 occur [33, 35].

$$O_2 + e_{aq}^- \longrightarrow O_2^{\bullet-} \quad (k = 1.9 \times 10^{10}\ M^{-1}\ s^{-1}) \quad (7)$$

$$O_2 + {}^{\bullet}H \longrightarrow HO_2^{\bullet} \quad (k = 2.1 \times 10^{10}\ M^{-1}\ s^{-1}) \quad (8)$$

$$O_2^{\bullet-} + H^+ \longrightarrow HO_2^{\bullet} \quad (k = 8 \times 10^{5}\ M^{-1}\ s^{-1}) \quad (9)$$

As can be seen, the reducing species $H^{\bullet}$ and e_{aq}^- are converted to $HO_2^{\bullet}$ and $O_2^{\bullet-}$ (Eq. 7 and 8), and $O_2^{\bullet-}$ is further converted to $HO_2^{\bullet}$. It can be concluded that under aerobic conditions the $HO_2^{\bullet}$ radicals are the dominant species in aqueous solution.

Under N_2O saturated conditions (anaerobic conditions), $^{\bullet}OH$ is the major reactive intermediate as e_{aq}^- converts to $^{\bullet}OH$ (Eq. 10):

$$e_{aq}^- + N_2O + H_2O \longrightarrow {}^{\bullet}OH + N_2 + OH^- \quad (10)$$

The relatively lower degradation of DOX in air compared to degradation in N_2O is due to the lower reactivity of $HO_2^{\bullet}$ compared to $^{\bullet}OH$ radicals.

During radiolysis of N_2 saturated aqueous solutions $^{\bullet}OH$ and e_{aq}^- are present and react with DOX. In general, a lower reactivity of e_{aq}^- toward DOX compared to $^{\bullet}OH$ radicals [24, 6] was observed under deaerated conditions.

Since e_{aq}^- and $^{\bullet}OH$ are the main reactive species under N_2 conditions, in order to study the influence of e_{aq}^- on DOX degradation it was necessary to remove $^{\bullet}OH$ from the system. This can be achieved by adding methanol, 2-PrOH, tert-butanol or thiourea which effectively remove $^{\bullet}OH$ [16, 24]. 2-PrOH is known to be a strong scavenger of $H^{\bullet}$ and $^{\bullet}OH$ by forming less reactive radical $^{\bullet}CH_2CCH_3OH$ according to the following equations:

$$^{\bullet}OH + (CH_3)_2COH \longrightarrow H_2O + {}^{\bullet}CH_2CCH_3OH \qquad k = 1{,}9 \times 10^9\ M^{-1}\ s^{-1} \quad (11)$$

$$H^{\bullet} + (CH_3)_2COH \longrightarrow H_2 + {}^{\bullet}CH_2CCH_3OH \qquad k = 7{,}4 \times 10^7\ M^{-1}\ s^{-1} \quad (12)$$

For that reason, we used 2-PrOH as a radical scavenger to investigate a possible reaction of e_{aq}^- with DOX. As can be seen from Fig. 3., the e_{aq}^- reacted with DOX but has the smallest effect on DOX degradation in comparison to other radicals.

On the other hand, thiourea is a fast scavenger of all three major radicals formed in the radiolysis of water, $^{\bullet}OH$, $H^{\bullet}$ and e_{aq}^-. The addition of thiourea almost completely retarded the degradation efficiency of DOX at the same absorbed dose. These experimental results indicated that primary reactive species ($H^{\bullet}$ and e_{aq}^-) are also involved in the degradation of DOX.

3.3. The influence of different inorganic ions on DOX degradation

It is known that inorganic salts can affect the efficiency of pollutants degradation [25, 36, 37], and have important influence on performance of AOPs [38]. In this part of the study NO_3^-, HPO_4^{2-} and HCO_3^- were chosen as the model radical scavengers to study their effect on DOX degradation behaviour. The results are shown in Fig. 4.

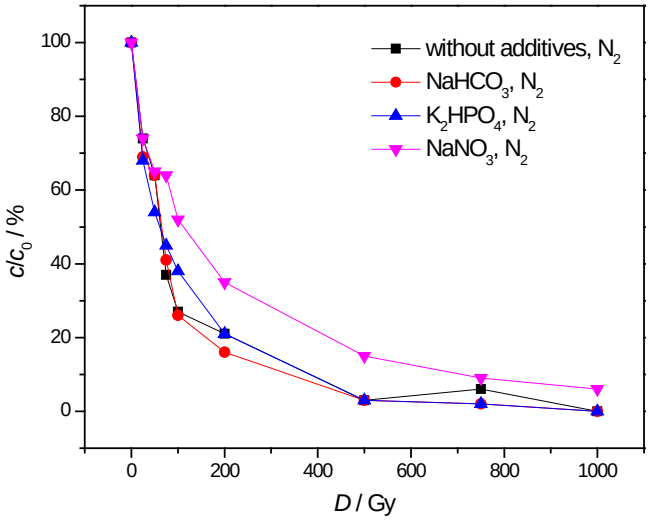

Figure 4. The effect of different inorganic ions on radiolytic degradation of DOX in N_2-saturated aqueous solution.

In a N_2-saturated solution in combination with NO_3^- ions at the irradiation dose of 200 Gy (Fig. 4) 65 % of DOX was degraded, which is much slower compared to aerobic (96 %) and N_2 conditions (76 %) (Fig. 3). However, the degradation was still much faster in comparison to those in N_2-saturated solution in combination with 2-PrOH (42 %) and thiourea (only 21 %). The different removal efficiency of DOX in the presence of investigated inorganic anions is due to their scavenging effect for reactive species such as $^{\bullet}OH$, e_{aq}^- and $^{\bullet}H$.

NO_3^- ions are scavengers of e_{aq}^-, as shown in equation (13) [34]. In addition, in aqueous solution HNO_3 can be easily produced (Eq. 14) which decrease the concentration of $H^{\bullet}$ and $^{\bullet}OH$ radicals (Eq. 15 and 16), finally resulting in a decrease of DOX radiolytic degradation. Furthermore, it has been reported that NO_3^- reacts very quickly with e_{aq}^- producing nitrite which could efficiently scavenge $^{\bullet}OH$ radicals [36].

$$NO_3^- + e_{aq}^- \longrightarrow NO_3^{2-} \quad (k = 9.7 \times 10^9\ M^{-1}\ s^{-1}) \quad (13)$$

$$H^+ + NO_3^- \longrightarrow HNO_3 \quad (k = (4.4\text{-}6.0) \times 10^8\ M^{-1}\ s^{-1}) \quad (14)$$

$$^{\bullet}OH + HNO_3 \longrightarrow H_2O + {}^{\bullet}NO_3 \quad (k = (0.88\text{-}1.2) \times 10^8\ M^{-1}\ s^{-1}) \quad (15)$$

$$^{\bullet}H + HNO_3 \longrightarrow H_2 + {}^{\bullet}NO_3 \quad (k = 1 \times 10^7\ M^{-1}\ s^{-1}) \quad (16)$$

HCO_3^- can react with $^{\bullet}OH$ radicals (Eq.17) to form $CO_3^{\bullet-}$ which has a lower redox potential (1.59 V) and higher selectivity compared to $^{\bullet}OH$ radicals. The high selectivity and longer lifetime of $CO_3^{\bullet-}$ in solution may lead to better removal performance in the degradation of organic pollutants [38]. HCO_3^- scavenges $^{\bullet}OH$ and e_{aq}^- by relatively slow reactions (Eq. 17 and 18):

$$^{\bullet}OH + HCO_3^- \longrightarrow CO_3^{\bullet-} + H_2O \quad (k = 1.0\times 10^7\ M^{-1}\ s^{-1}) \qquad (17)$$

$$e_{aq}^- + HCO_3^- \longrightarrow \text{products} \quad (k = 1.0\times 10^6\ M^{-1}\ s^{-1}) \qquad (18)$$

Since these reactions are quite slow and the reaction rate of $CO_3^{\bullet-}$ with organic pollutants is lower than that of $^{\bullet}OH$, HCO_3^- ions had no effect on the degradation of DOX. Thus, organic pollutant degradation occurred by hydroxyl radicals.

Phosphate ions in solution can exist in various forms and the reaction rates between $^{\bullet}OH$ and different phosphate ions can be significantly different. During ionizing irradiation HPO_4^{2-} reacts with $^{\bullet}OH$ radicals forming $HPO_4^{\bullet-}$ at a rate constant of $1.5 \times 10^5\ M^{-1}\ s^{-1}$ which is slow enough not to affect degradation of DOX. Despite this result, the reactivity of phosphate radicals for aromatic compounds is comparable with $^{\bullet}OH$ so their contribution in the removal of organic pollutants in real water matrices should not be neglected.

As far as the effect of tested inorganic anions is concerned the presence of NO_3^- most strongly affected the removal efficiency of DOX compared with other ions tested. The relatively higher inhibition in the presence of NO_3^- could be due to the high rate constant of $^{\bullet}OH$ radical with NO_3^- leaving relatively less $^{\bullet}OH$ for reaction with DOX. However, at an absorbed dose of 1000 Gy almost 99 % of DOX was degraded regardless of the presence of inorganic ions indicating that the reaction of $^{\bullet}OH$ oxidation and direct decomposition contributed to the degradation of DOX.

To investigate the effect of water components on the removal of DOX by radiation the underground water was used. Real water samples such as groundwater are characterized by a complex composition. The dissolved organic substances could compete with the target pollutant for reactive species that are formed during irradiation and accelerate or slow down degradation [25]. Ultrapure water and groundwater samples containing equal concentrations of DOX were purged with N_2 and irradiated with a dose ranging from 25 Gy to 1000 Gy (Fig. 5). The dose constant, *k*, was determined by considering that pollutant degradation kinetic data fits a pseudo-first order kinetics (Fig. 6). The results revealed that the degradation of DOX in groundwater was significantly slower than in ultrapure water, which was expected based on

the results presented in Fig. 4. One explanation for this decrease in the dose constant is that the species produced by radiolysis also react with other solutes in the medium, including dissolved organic matter and inorganic compounds present in groundwater. Ocampo-Perez and co-authors [25] reported that the rate constant for degradation of cytarabine by gamma irradiation was lower in groundwater and surface water and significantly lower in wastewater than in ultrapure water. A similar trend was observed for the degradation of metronidazole [39], cytarabine [25] and diphenolic acid [40] in different types of water matrix.

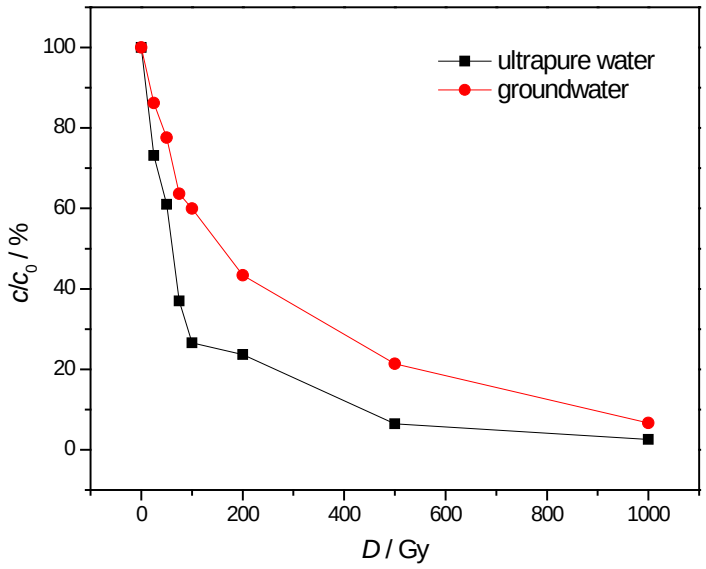

Figure 5. The influence of water matrix on the degradation of DOX.

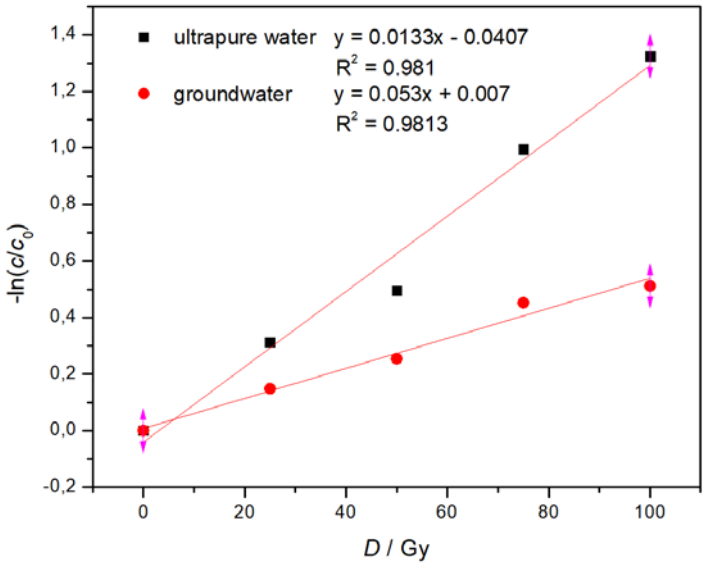

Figure 6. Degradation kinetics of DOX in aqueous solution.

3.4. The effect of solution pH on degradation of DOX

The *G*-values of the reactive species formed during water radiolysis depend on the pH of the solution. The pH value of the DOX water solution was 6.5, without adjustment. The desired pH values of 3.5 and 9.5 were prepared by adding hydrochloric acid or sodium hydroxide before the irradiation process. The fastest degradation occurred at pH 6.5 (84 %) at an absorbed dose of 200 Gy, while it was 71 % at pH 9.5 and 75 % at pH 3.4 (Fig. 7). The results show that DOX degraded the most at approximately neutral pH, which is probably due to higher concentration of $^{\bullet}OH$ and $O_2^{\bullet-}$ radicals at this pH. In alkaline solution, especially above pH 10 less reactive $O^{\bullet-}$ species are formed and the concentration of $^{\bullet}H$ and $^{\bullet}OH$ is reduced (Eq. 19 and 20) causing the $^{\bullet}OH$ concentrations to decrease and resulting in lower degradation efficiency.

$$^{\bullet}OH + {}^{-}OH \longrightarrow O^{\bullet-} + H_2O \qquad k = 1.3 \times 10^{10}\ M^{-1}\ s^{-1} \qquad (19)$$

$$^{\bullet}H + {}^{-}OH \longrightarrow e_{aq}^{-} + H_2O \qquad k = 2.2 \times 10^{7}\ M^{-1}\ s^{-1} \qquad (20)$$

Under acidic conditions following reaction (21) occurs:

$$e_{aq}^{-} + H^{+} \longrightarrow {}^{\bullet}H \qquad k = 2.3 \times 10^{10}\ M^{-1}\ s^{-1} \qquad (21)$$

The conversion of e_{aq}^{-} to $^{\bullet}H$ (Eq. 21) prevented the reaction of e_{aq}^{-} and $^{\bullet}OH$ (Eq. 6) leaving more $^{\bullet}OH$ radicals to react with target pollutant.

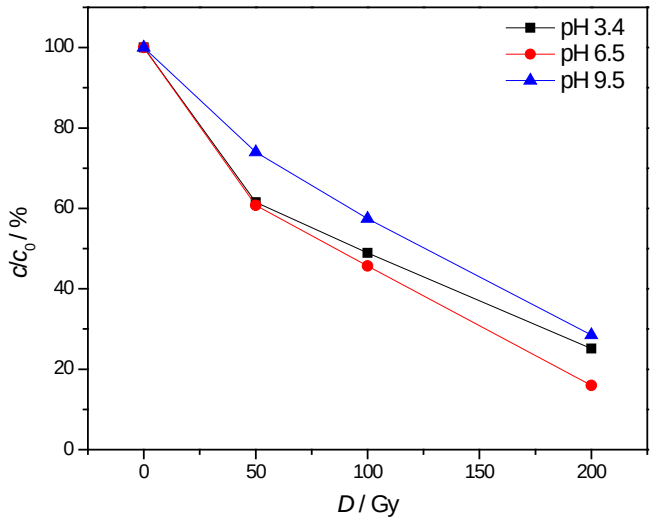

Figure 7. The influence of pH on radiolytic degradation of DOX .

3.5. Identification of products by LC/MS measurements

Aqueous solutions of DOX were irradiated with 50 Gy (P = 0.54 Gy s^{-1}) in the presence of air and N_2O and analyzed by LC-HRMS. The degradation products were detected, and their structures were suggested based on their tandem mass spectra (table SI1 in SI). Collision-induced dissociation (CID) was performed at three different collision energies (CE), and the *m/z* values and corresponding relative intensities of the fragment ions are listed in Tables SI2 – 15 in SI. The degradation pathways are shown in Schemes 1 and 2.

A chromatographic peak belonging to protonated DOX (*m/z* 452.1928) was found in both samples, at a retention time of 5.9 min. The MS/MS analysis revealed two possible pathways of fragmentation of the molecule, by bond breaking of the piperazine ring, giving ions of *m/z* 247, 233, 231, and 220, and by bond breaking between the piperazine ring and the benzodioxane moiety, giving ions at *m/z* 163, 135 and 289. However, the main fragmentation pathway was bond breakage in the dioxane ring, which formed an ion at *m/z* 344. These ions are characteristic in the CID spectra of DOX and can also be found in the CID spectra of most of its degradation products, depending on their structure. Based on these spectra, fragmentation pathways of DOX and its degradation products were proposed and can be found in SI (Figures SI2 – 12). The proposed structures of the fragment ions of DOX are consistent with the literature [41, 42] However, it should be noted that both ESI [42] and EI [41] ionization modes were used.

Analysis of the two irradiated samples showed a similar set of degradation products, with some differences. The chromatographic peak at a retention time of 1.3 min can be assigned to compound 1 with a molecular ion of *m/z* 394 and molecular formula $C_{17}H_{23}N_5O_6$. Compound 2 of *m/z* 378 and molecular formula $C_{17}H_{23}N_5O_5$ (retention time 1.7 min) may be treated as a primary product of transformation. Its formation involves the cleavage of the dioxane moiety. Its further hydroxylation results in formation of compound 1.

The ion of *m/z* 468 appeared at four retention times in both samples, although only one isomer dominated in the sample irradiated in the presence of air, whereas all four were equally prevalent in the sample irradiated in the presence of N_2O (Fig. 8). These compounds correspond to monohydroxylated DOX, and MS/MS analysis of these compounds can provide some insight into their structures (Fig. 9 and Tables SI6, 7, 8 and 15 in SI). Compound 4 with a retention time of 4.2 is formed by hydroxylation of the piperazine ring, which can be confirmed by the presence of ions *m/z* 135, 360, 342, and 450. Compounds 5a and 5b are formed by

hydroxylation of the aromatic ring of the benzodioxane moiety. This was confirmed by MS/MS analysis as ions of *m/z* 135 and 163 corresponding to the benzodioxane moiety were not observed. Also, the presence of ions of *m/z* 344 and 290 confirms that hydroxylation didn't occur at the piperazine moiety. The differences in retention times (4.5 min and 4.9 min) could be due to the position of the hydroxyl group. Another monohydroxylated product, compound 10, was found with a retention time of 5.7 min. The MS/MS analysis indicates hydroxylation of the piperazine ring, due to the presence of ions of *m/z* 360, 342 and 306. The longer retention time can be explained by the formation of hydrogen bonds between the hydroxyl group and a carbonyl group. It is known that the formation of intramolecular hydrogen bonds leads to a decrease in solute-solvent association, causing the increase in solute-stationary phase association, and therefore longer retention times [43, 44].

Compounds 6a and 6b were found in both samples and correspond to addition of water molecule to the double bond in benzene ring with destruction of aromaticity. According to the CID spectra, the hydroxylation occurred on the aromatic ring of the benzodioxane moiety. The presence of two chromatographic peaks indicates different positions of the hydroxyl group. Compound 3 of *m/z* 486 corresponds to a dihydroxylated and reduced product in which both hydroxyl groups are located in the piperazine ring. Its possible non-reduced precursor of *m/z* 484 with two hydroxyl groups was not detected in the TIC chromatogram. However, extracted ion chromatogram based on the current of *m/z* 484.1825 ion demonstrated a number of peaks with various retention times (Figure SI1). It is rather logical as each of four detected primary hydroxylated products (ions of *m/z* 468) can further react with introduction of the second oxygen atom into the molecule. Since the forming compounds are rather reactive their levels are rather low.

Compounds 8a and 8b, with retention times of 5.3 and 5.5 min, correspond to products with one hydrolyzed methoxy group. The structures of these products are confirmed by MS/MS analysis where ions were observed at *m/z* 233, 207, 330, 231, 276, and 220. Small differences in retention times suggest that the position of the hydroxyl group may affect the polarity of the compounds and their retention times.

Two other degradation products were found only in the sample irradiated in the presence of air. Compound 7 may be formed by the partial rupture of the piperazine moiety, and compound 9 may be formed from compound 4 by elimination of water molecule from the piperazine cycle.

The presence of ions of *m/z* 163 and 342 in the CID spectra of compound 9 confirms the presence of the original carbonyl group.

Since compounds 2 (in air) and 5 (in N_2O) were the most abundant, we proposed a mechanism for their formation in Scheme 3. For the formation of compound 2, a ring cleavage of 1,4 dioxane with the elimination of o-dihydroquinone is proposed. On the other hand, compound 5 was formed by addition of •OH to the aromatic ring.

Comparing the degradation products obtained by gamma irradiation with the previously reported [29] degradation products obtained by UVA and UVC irradiation, significant differences can be observed. Only compounds 2 and 5 obtained under gamma irradiation conditions were also found under photolytic conditions. Compounds 6 and 7 obtained under gamma irradiation conditions had exactly the same mass and molecular formula as the corresponding compounds found under photolytic conditions, but MS/MS analysis showed differences in the structures. All other compounds found under gamma irradiation conditions were new, and were not observed under UV irradiation conditions.

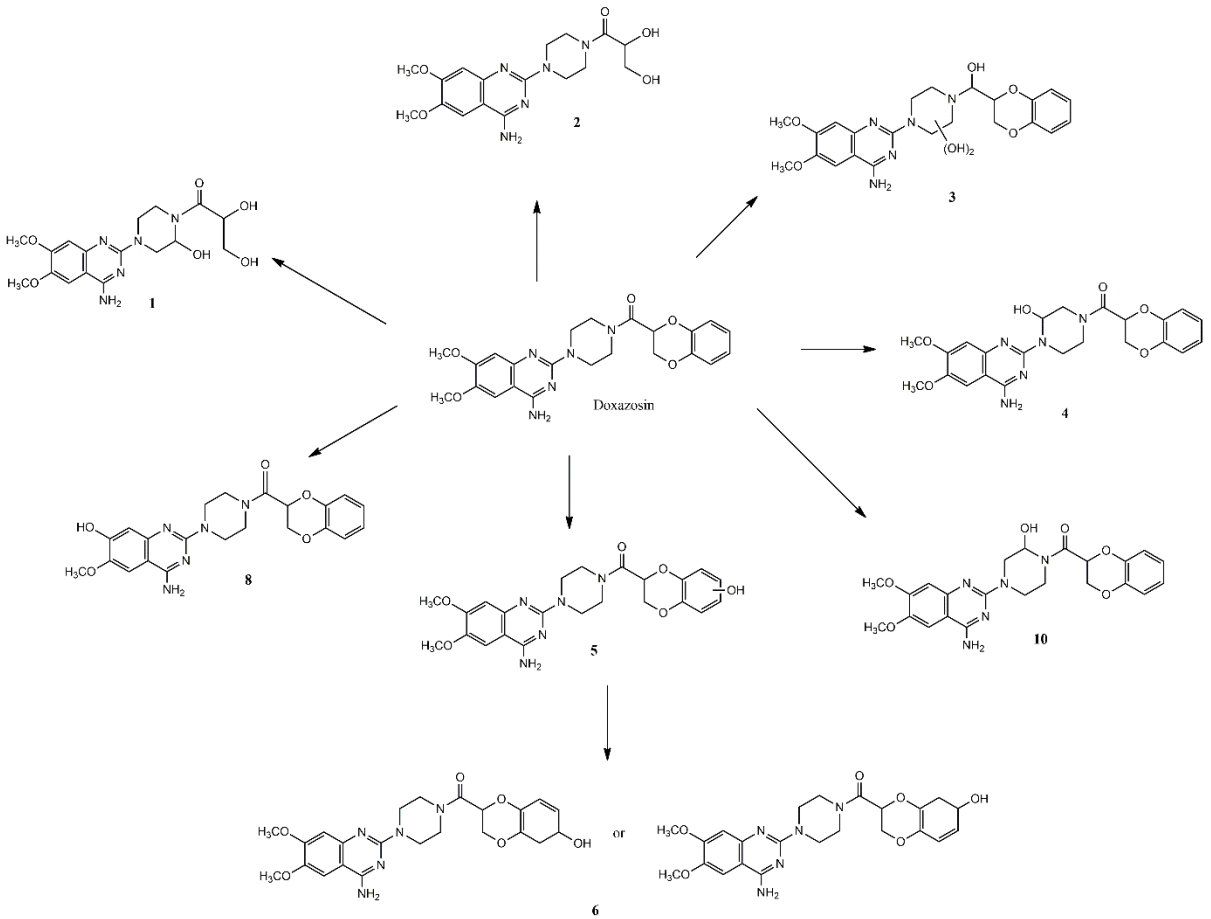

Scheme 1. Proposed degradation pathway of DOX under gamma irradiation in the presence of N_2O.

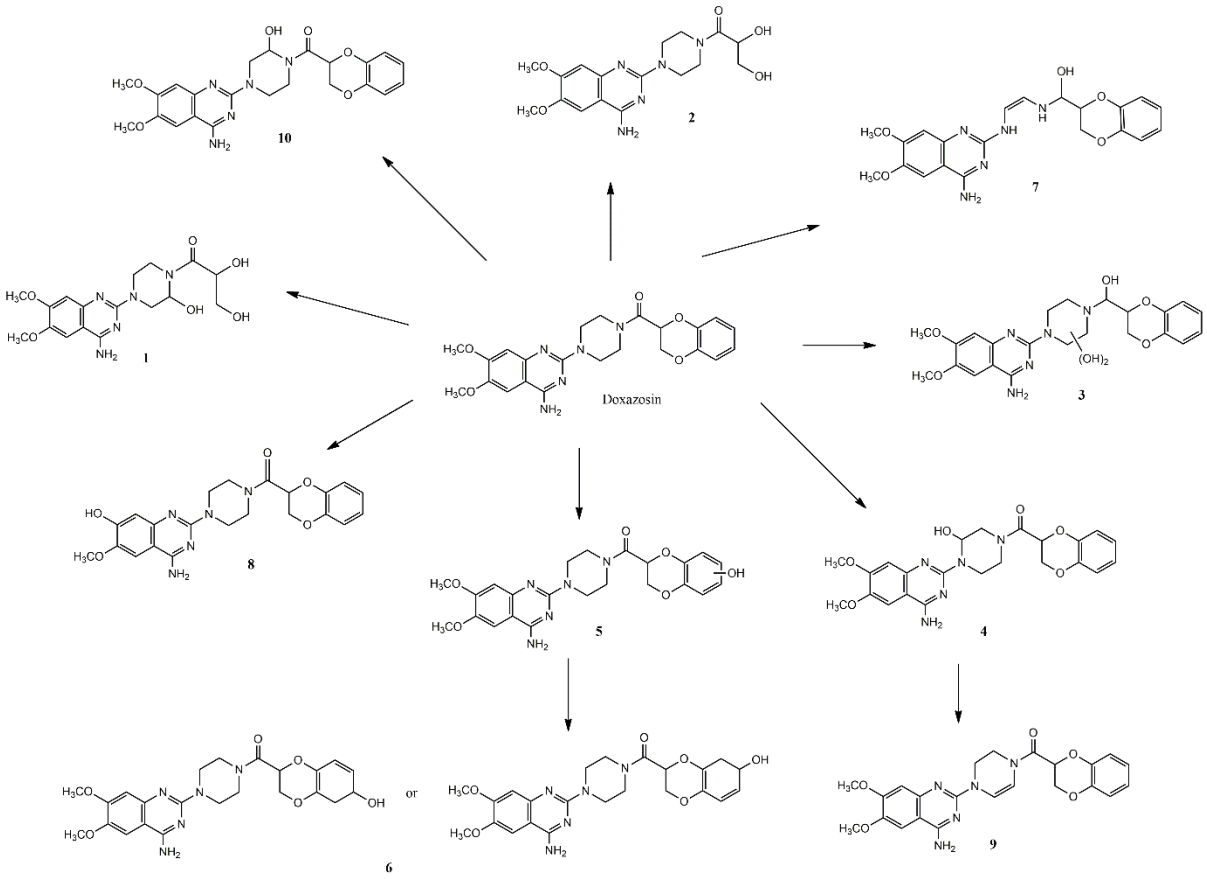

Scheme 2. Proposed degradation pathway of DOX under gamma irradiation in the presence of air.

a)

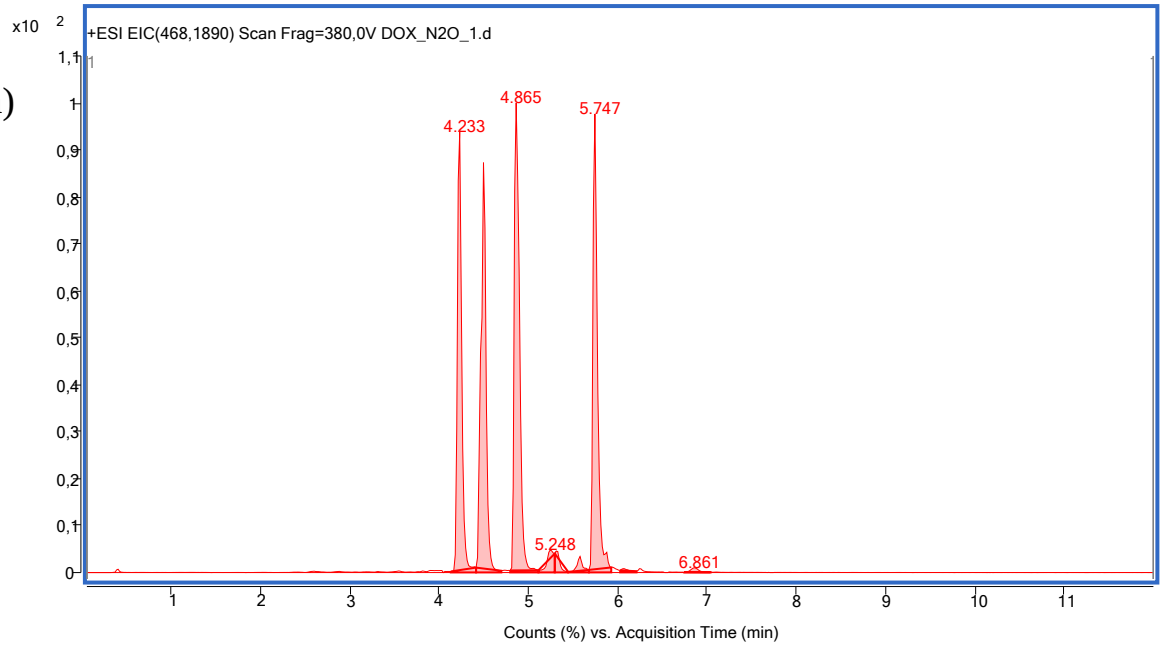

b)

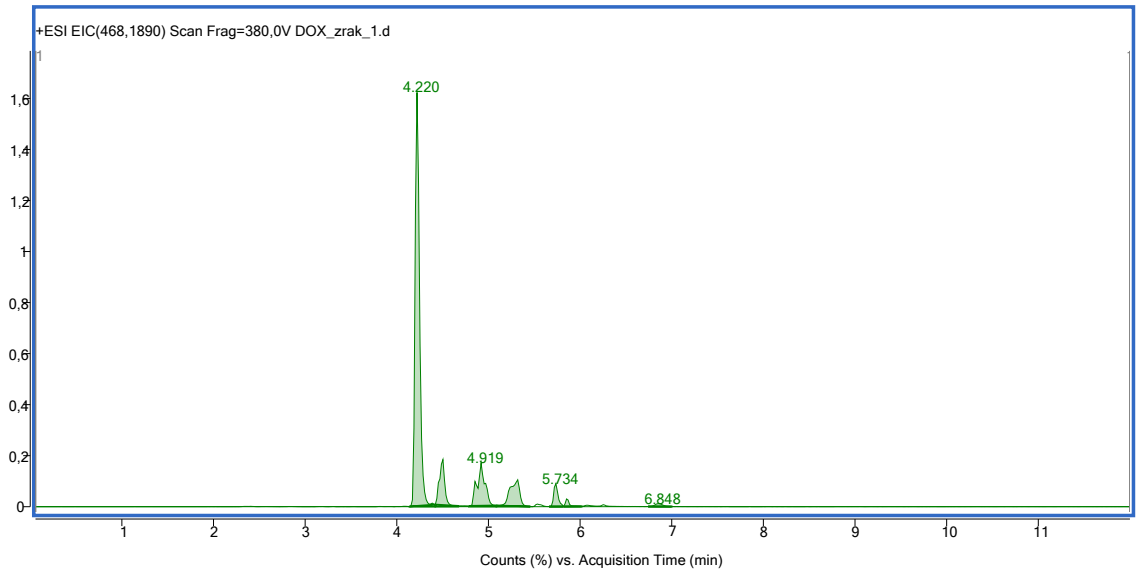

Figure 8. Extracted ion chromatograms (*m/z* 468.1890) for monohydroxylated DOX obtained under gamma irradiation in the presence of N_2O (a) and air (b).

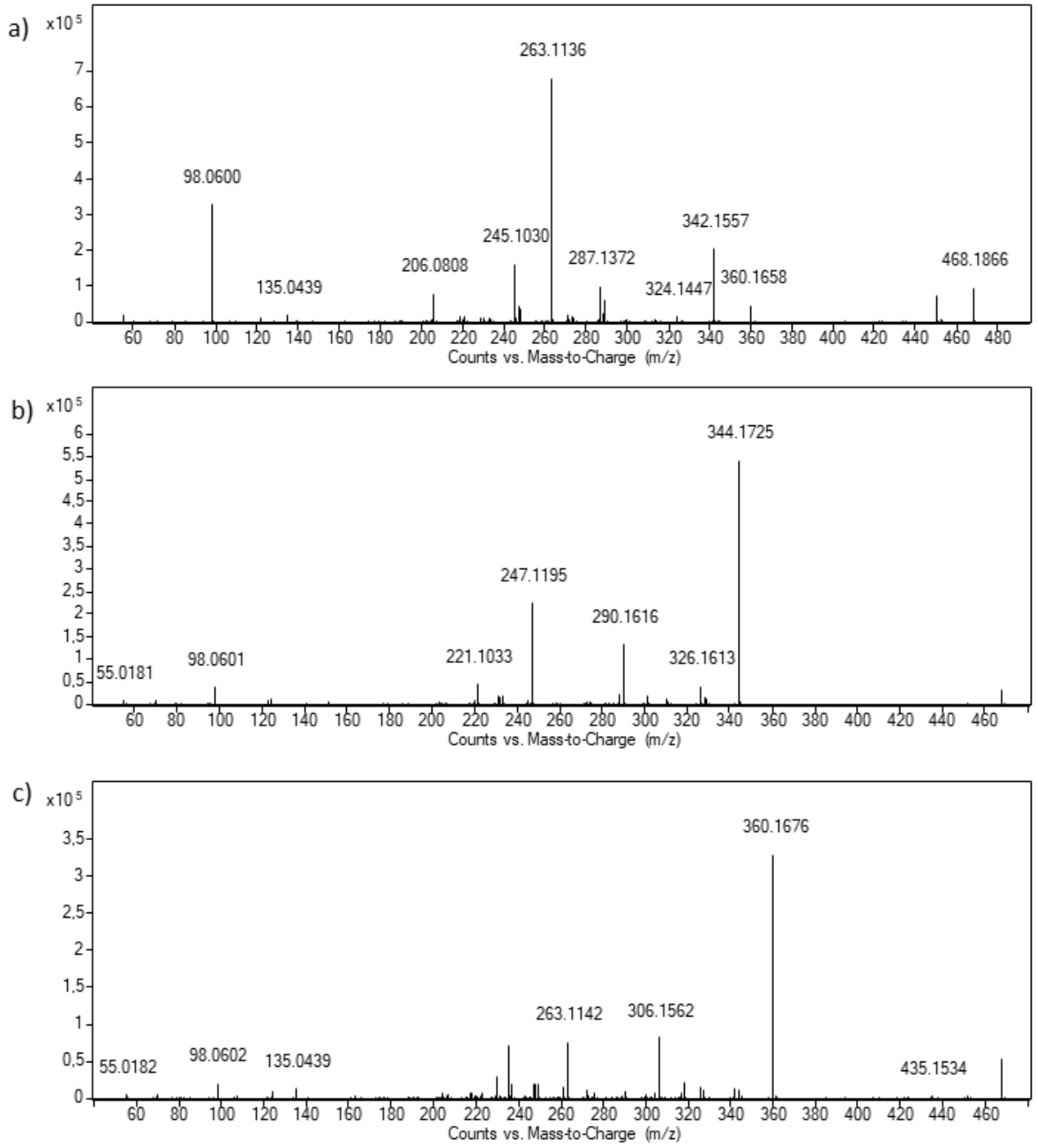

504

505 Figure 9. CID tandem mass spectra of compound 4 (a), 5a (b) and 10 (c) under CE 40 V
506 conditions.

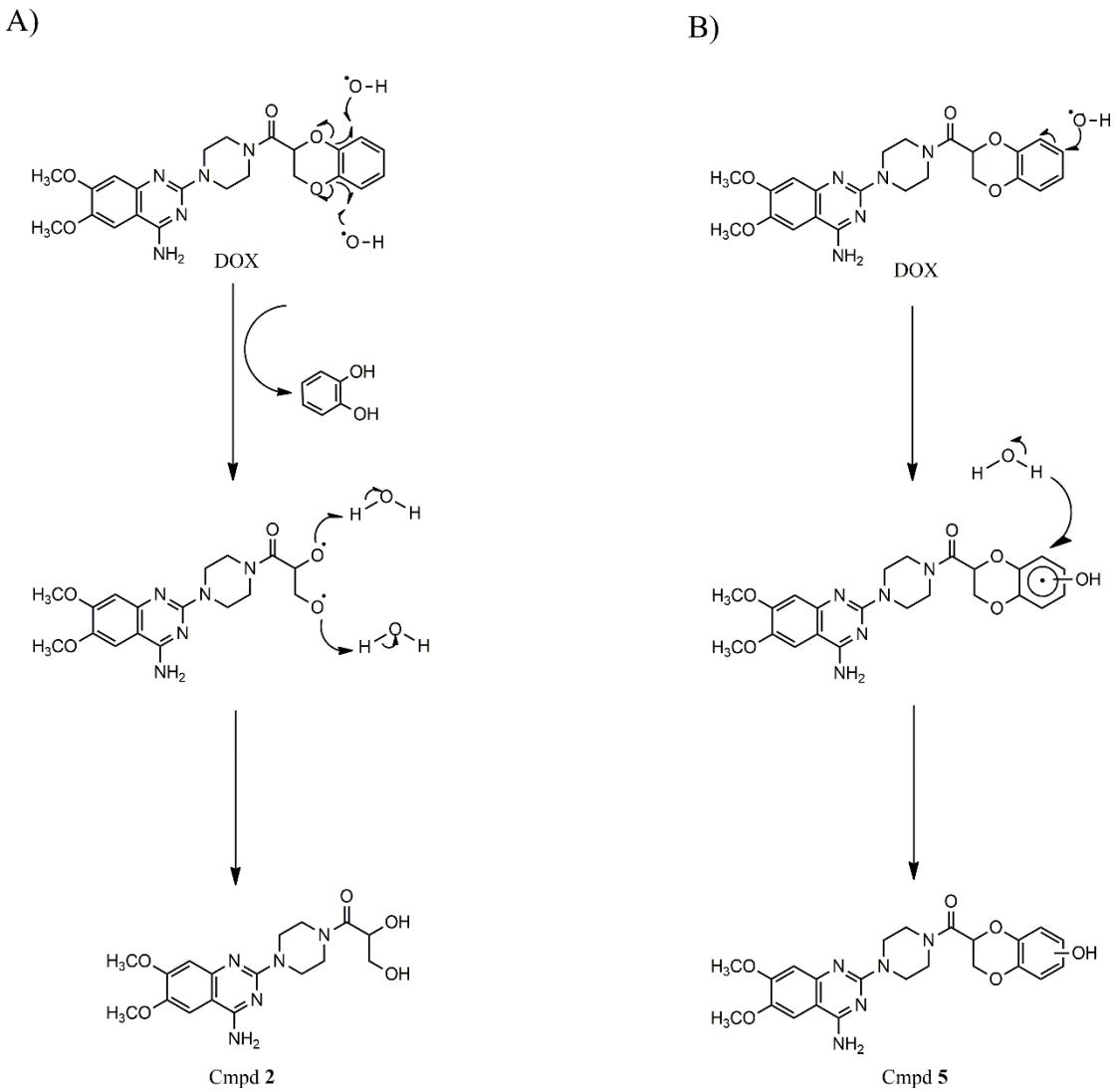

Scheme 3. Proposed mechanism of formation of the most common degradation products after gamma irradiation of DOX in air (A) and in N_2O (B).

3.6. DOC analysis of aqueous DOX solution and toxicity

The efficiency of radiolysis of DOX depends not only on the effectiveness of degradation but also on the mineralization of the parent compound. DOC removal was evaluated to assess the mineralization efficiency of DOX in an aqueous solution. DOC value decreased when irradiation dose was increased. A reduction of 10, 34, and 60 % of DOC was observed when the irradiation dose was increased from 1 to 10 kGy (Fig. 10). The results indicate that despite the strong degradation of DOX at low irradiation doses, higher doses are required for the overall mineralization process. Higher mineralization occurs due to the degradation of the formed intermediates of DOX as the absorbed dose increases.

In many cases, extremely high absorbed doses are required to achieve complete mineralization [45], which is not cost-effective for practical use. To overcome the drawbacks of single AOP, ionizing radiation is therefore often combined with other methods such as H_2O_2, ozone or subsequent biological treatment to improve the effectiveness of degradation and reduce costs [46, 47].

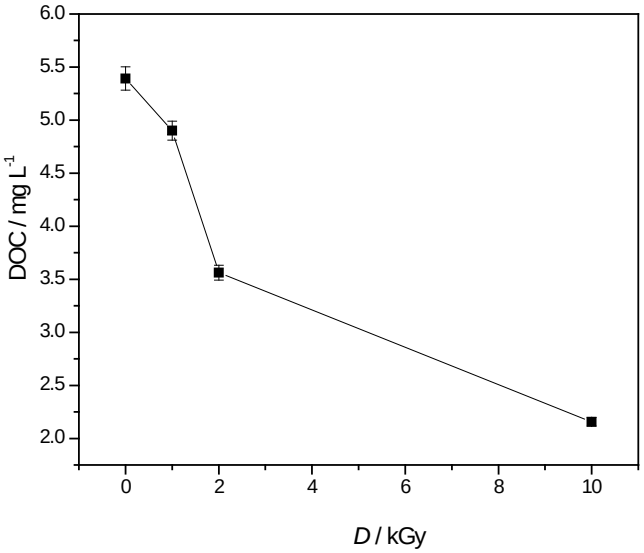

Figure 10. The influence of irradiation dose on DOC.

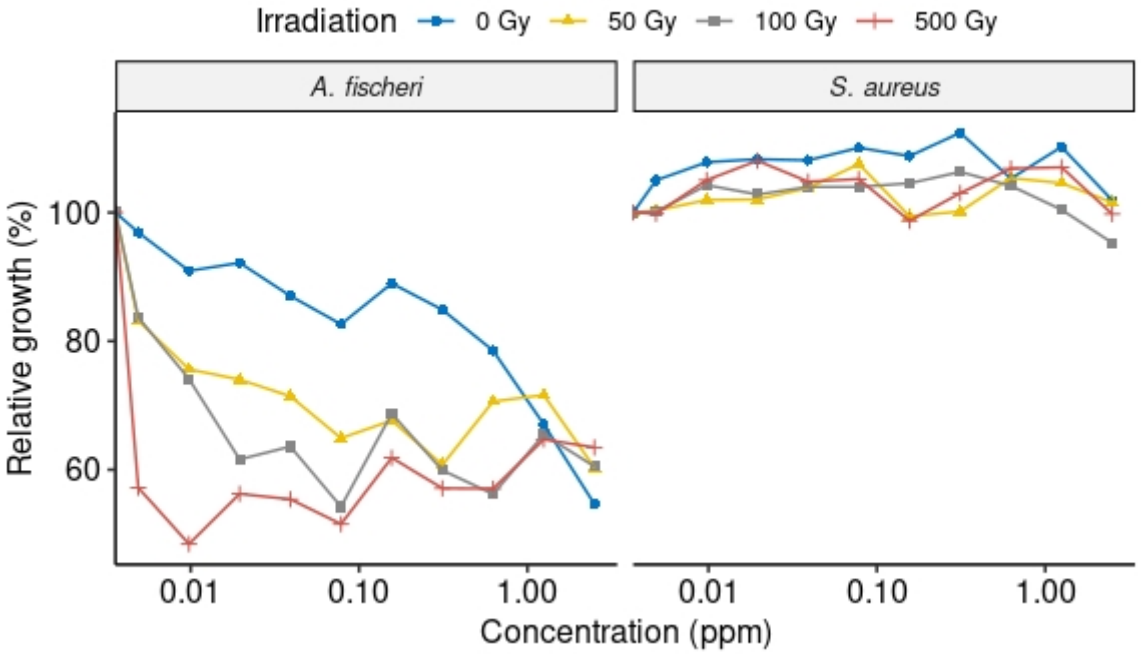

Figure 11. The influence of irradiated DOX aqueous solution on the relative growth of *V. fischeri* and *S. Aureus.*

In addition to the degree of mineralization as a measure of the effectiveness of the applied AOP process, another important factor is the change in toxicity during irradiation. Generally, treatment with different AOPs can affect the toxicity of organic products by changing the structure of the parent compound and forming by-products with a lower molecular weight [48, 49, 50, 51, 52]. As shown in Fig. 11 there was no complete inhibition of the relative growth of *V. fischeri* and S. *aureus*. *V. fischeri* was more sensitive to the presence of DOX. Partial growth inhibition was observed in the control sample (0 Gy) in a dose-dependent manner with a ceiling effect of growth inhibition of approximately 40-50 % relative to the growth control sample. A similar effect was observed in irradiated samples, particularly in *V. fischeri* where the ceiling effect was predominant even at low DOX concentrations. Under higher irradiation dose (500 Gy) DOX was no longer detected and the toxicity could correspond to the by-products. In general, samples irradiated at higher doses were more toxic than those irradiated at lower doses [53].

4. Conclusions

The present work shows that gamma irradiation is very efficient and promising technology for the effective removal of DOX in aqueous solution. The high removal efficiency of DOX under N_2O (> 99 %) and under air (80 %) at dose of 100 Gy were accompanied with low degree of mineralization (10 % at dose of 1 kGy). Despite the strong degradation of DOX up to 200 Gy, much higher doses are required for the overall mineralization process. In the absence of inorganic anions $^{\bullet}OH$ was the predominant radical species responsible for DOX degradation during gamma irradiation. The degradation of DOX was less efficient in the presence of NO_3^- and especially in underground water due to the presence of organic matter and various inorganic ions. DOX degradation was favorable in the neutral, slightly acidic range (pH = 6.5) and decreased under acidic or alkaline conditions. Samples irradiated with 500 Gy resulted in higher toxicity testing on *V. fischeri* bacteria than samples irradiated with lower doses.

LC-HRMS/MS analyses allowed the identification of 9 degradation products in N_2O saturated aqueous DOX solution and additional two in equilibrium with air. Detailed degradation pathways have been proposed.

Acknowledgments

This work was supported by the project CIuK co-financed by the Croatian Government and the European Union through the European Regional Development Fund-Competitiveness and Cohesion Operational Programme (Grant KK.01.1.1.02.0016.).

References

[1] M. Klavarioti, D. Mantzvinos, D. Kassinos, Removal of residual pharmaceuticals from aqueous systems by advanced oxidation processes, Environ. Int. 35 (2009) 402–417, https://doi.org/10.1016/j.envint.2008.07.009.

[2] C. Nebot, R. Falcon, K. G. Boyd, S. W. Gibb, Introduction of human pharmaceuticals from wastewater treatment plants into the aquatic environment: a rural perspective, Environ. Sci. Pollut. Res. 22 (2015) 10559–10568, https://doi.org/10.1007/s11356-015-4234-z.

[3] M. Sayed, P. Fu, L. A. Shah, M. H. Khan, J. Nisar, M. Ismael, P. Zhang, VUV-Photocatalytic Degradation of Bezafibrate by Hydrothermally Synthesized Enhanced {001} Facets TiO2/Ti Film, J. Phys. Chem. A. 120 (2016.) 118–127, https://doi.org/10.1021/acs.jpca.5b10502.

[4] M. Huerta-Fontela, M. T. Galceran, F. Ventura, Occurrence and removal of pharmaceuticals and hormones through drinking water treatment, Water Res. 45 (2011) 1432–1442, https://doi.org/10.1016/j.watres.2010.10.036.

[5] T. Csay, G. Racz, E. Takács, L. Wojnárovits, Radiation induced degradation of pharmaceutical residues in water: Chloramphenicol, Rad. Phys. Chem., 81 (2012) 1489–1494, https://doi.org/10.1016/j.radphyschem.2012.01.021.

[6] J. Wang, L. J. Xu, Advanced Oxidation Processes for Wastewater Treatment: Formation of Hydroxyl Radical and Application, Crit. Rev. Environ. Sci. Technol. 42 (2012) 251–325, https://doi.org/10.1080/10643389.2010.507698.

[7] S. Pandey, N. Son, S. Kim, D. Balakrishnan, M. Kang, Locust Bean gum-based hydrogels embedded magnetic iron oxide nanoparticles nanocomposite: Advanced materials for environmental and energy applications, Environ. Res. 214 (2022) 114000, https://doi.org/10.1016/j.envres.2022.114000.

[8] S. Pandey, N. Son, M. Kang, Synergistic sorption performance of karaya gum crosslink poly(acrylamide-co-acrylonitrile) @ metal nanoparticle for organic pollutants, Int. J. Biol. Macromol. 210 (2022) 300–314, https://doi.org/10.1016/j.ijbiomac.2022.05.019.

[9] Gupta, C. Pandit, S. Pandit, P. K. Gupta, D. Lahiri, D. Agarwal, S. Pandey, Potential and future prospects of biochar-based materials and their applications in removal of organic contaminants from industrial wastewater. J. Mater. Cycles Waste Manag. 24 (2022) 852–876, https://doi.org/10.1007/s10163-022-01391-z.

[10] M. Khapre, A. Shekhawat, D. Saravanan, S. Pandey, R. Jugade, Mesoporous Fe–Al-doped cellulose for the efficient removal of reactive dyes, Mater. Adv. 3 (2022) 3278–3285, https://doi.org/10.1039/D2MA00146B.

[11] A. J. Ebele, M. A. E. Abdallah, S. Harrad, Pharmaceuticals and personal care products (PPCPs) in the freshwater aquatic environment, Emerg. Contam. 3 (2017) 1–16, https://doi.org/10.1016/j.emcon.2016.12.004.

[12] H. Ryu, B. Li, S. de Guise, J. McCutcheon, Y. Lei, Recent progress in the detection of emerging contaminants PFASs, J. Hazard. Mater. 408 (2021) 124437, https://doi.org/10.1016/j.jhazmat.2020.124437.

[13] B. Petrie, R. Barden, B. Kasprzyk-Hordern, A Review on Emerging Contaminants in Wastewaters and the Environment: Current Knowledge, Understudied Areas and Recommendations for Future Monitoring, Water Res. 72 (2015) 3−27, https://doi.org/10.1016/j.watres.2014.08.053.

[14] M. Patel, R. Kumar, K. Kishor, T. Mlsna, C. U. Pittman, D. Mohan, Pharmaceuticals of Emerging Concern in Aquatic Systems: Chemistry, Occurrence, Effects, and Removal Methods, Chem. Rev. 119 (2019) 3510–3673. https://doi.org/10.1021/acs.chemrev.8b00299.

[15] B. Halling-Sørensen, S. N. Nielsen, P. Lanzky, F. Ingerslev, H. H. Lützhøft, S. Jørgensen, Occurrence, Fate and Effects of Pharmaceutical Substances in the Environment-A Review, Chemosphere 36 (1998) 357−393, https://doi.org/10.1016/S0045-6535(97)00354-8.

[16] J. Wang, R. Zhuan, L. Chu, The occurrence, distribution and degradation of antibiotics by ionizing radiation: An overview, Sci. Total Environ. 646 (2019) 1385–1397, https://doi.org/10.1016/j.scitotenv.2018.07.415.

[17] L. Chu, J. Wang, Degradation of 3-chloro-4-hydroxybenzoic acid in biological treated effluent by gamma irradiation, Radiat. Phys. Chem. 119 (2016) 194–199, https://doi.org/10.1016/j.radphyschem.2015.10.016.

[18] A. Tegzea, G. Ságia, K. Kovács, R. Homlok, T. Tóth, C. Mohácsi-Farkas, L. Wojnárovits, E. Takács, Degradation of fluoroquinolone antibiotics during ionizing radiation treatment and assessment of antibacterial activity, toxicity and biodegradability of the products, Rad. Phys. Chem. 147 (2018) 101–105, https://doi.org/10.1016/j.radphyschem.2018.02.015.

[19] A. Tegzea, G. Sági, K. Kovács, T. Tóth, E. Takác, L. Wojnárovits, Radiation induced degradation of ciprofloxacin and norfloxacin: Kinetics and product analysis, Rad. Phys. Chem. 158 (2019) 68–75, https://doi.org/10.1016/j.radphyschem.2019.01.025.

[20] J. Wang, S. Wang, Effect of inorganic anions on the performance of advanced oxidation processes for degradation of organic contaminants, Chem Eng. J. 411 (2021) 128392, https://doi.org/10.1016/j.cej.2020.128392.

[21] S. Wang, J. Wang, Electron Beam Technology Coupled to Fenton Oxidation for Advanced Treatment of Dyeing Wastewater: From Laboratory to Full Application, ACS EST Water 2 (2022) 852–862, https://doi.org/10.1021/acsestwater.2c00040.

[22] J. J. Wang, R. Zhuan, Oxidative removal of carbamazepine by peroxymonosulfate (PMS) combined to ionizing radiation: Degradation, mineralization and biological toxicity, Sci. Total Environ. 658 (2019) 1367–1374, https://doi.org/10.1016/j.scitotenv.2018.12.304.

[23] J. Wang, L. Chu, Irradiation treatment of pharmaceutical and personal care products (PPCPs) in water and wastewater: An overview, Rad. Phys. Chem., 125 (2016) 56–64, https://doi.org/10.1016/j.radphyschem.2016.03.012.

[24] J. Nisar, M. Sayed, F. U. Khan, H. M. Khan, M. Iqbal, R. A. Khan, M. Anas, Gamma–irradiation induced degradation of diclofenac in aqueous solution: Kinetics, role of reactive

655 species and influence of natural water parameters, J. Environ. Chem. Eng. 4 (2016) 2573–2584,
656 https://doi.org/10.1016/j.jece.2016.04.034.

657 [25] R. Ocampo-Perez, J. Rivera-Utrilla, M. Sanchez-Polo, J. J. Lopez-Pe˜nalver, R. Leyva-
658 Ramos, Degradation of antineoplastic cytarabine in aqueous solution by gamma radiation,
659 Chem. Eng. J. 174 (2011) 1–8, https://doi.org/10.1016/j.cej.2011.07.017.

660 [26] D. Kanakaraju, B. D. Glass, M. Oelgemöller, Advanced oxidation process-mediated
661 removal of pharmaceuticals from water: a review, J. Environ. Manag. 219 (2018) 189–207,
662 https://doi.org/10.1016/j.jenvman.2018.04.103.

663 [27] J. Karpinska, A. Sokol, J. Koldys, A. Ratkiewicz, Studies on the kinetics of doxazosin
664 degradation in simulated environmental conditions and selected advanced oxidation processes,
665 Water 11 (2019) 1–16, https://doi.org/10.3390/w11051001.

666 [28] A. Piecha, M. Sarakha, P. Trebše, Photocatalytic degradation of cholesterol-lowering
667 statin drugs by TiO2-based catalyst. Kinetics, analytical studies and toxicity evaluation, J.
668 Photochem. Photobiol. A 213 (2010) 61–69,
669 https://doi.org/10.1016/j.jphotochem.2010.04.020.

670 [29] I. Tartaro Bujak, M. Bavcon Kralj, D. S. Kosyakov, N. V. Ul'yanovskii, A. T. Lebedev,
671 P. Trebše, Photolytic and photocatalytic degradation of doxazosin in aqueous solution, Sci.
672 Total Environ. 740 (2020) 140131–140138, https://doi.org/10.1016/j.scitotenv.2020.140131.

673 [30] M. Majer, M. Roguljić, Ž. Knežević, A. Starodumov, D. Ferenček, V. Brigljević, B.
674 Mihaljević, Dose mapping of the panoramic 60Co gamma irradiation facility at the Ruđer
675 Bošković Institute – Geant4 simulation and measurements, Appl. Radiat. Isot. 154 (2019)
676 108824, https://doi.org/10.1016/j.apradiso.2019.108824.

677 [31] I. Ciglenečki, I. Vilibić, J. Dautović, V. Vojvodić, B. Ćosović, P. Zemunik, H. Mihanović,
678 Dissolved organic carbon and surface active substances in the northern Adriatic Sea: Long-
679 term trends, variability and drivers, Sci. Total Environ. 730 (2020) 139104,
680 https://doi.org/10.1016/j.scitotenv.2020.139104.

681 [32] CLSI. Methods for Dilution Antimicrobial Susceptibility Tests for Bacteria That Grow
682 Aerobically, 10th ed.; M07-A10; Clinical and Laboratory Standards Institute: Wayne, PA,
683 USA, 2015.

684 [33] A. A. Basfar, H. M. Khan, A. A. Al-Shahrani, W. J. Cooper, Radiation induced
685 decomposition of methyl tert-butyl ether in water in presence of chloroform: Kinetic modelling,
686 Water Res.39 (2005) 2085–2095, https://doi.org/10.1016/j.watres.2005.02.019.

687 [34] G. V. Buxton, C. L. Greenstock, W. P. Helman, A. B. Ross, Critical review of rate
688 constants for reactions of hydrated electrons, hydrogen atoms and hydroxyl radicals (•OH/•O−)
689 in aqueous solution, J. Phys. Chem. 17 (1988) 513–886, https://doi.org/10.1063/1.555805.

690 [35] Spinks, J. W. T., Wood, R. J. 1990. Introduction to Radiation Chemistry, Wiley, New
691 York.

692 [36] J. A. Khan, N. S. Shah, H. M. Khan, Decomposition of atrazine by ionizing radiation:
693 Kinetics, degradation pathways and influence of radical scavengers, Sep. Purif. Technol. 156
694 (2015) 140–147, https://doi.org/10.1016/j.seppur.2015.09.064.

[37] L. Wojnarovits, E. Takacs, Wastewater treatment with ionizing radiation, J. Radioanal. Nucl. Chem. 311 (2017) 973–981, https://doi.org/10.1007/s10967-016-4869-3.

[38] J. Wang, S. Wang, Effect of inorganic anions on the performance of advanced oxidation processes for degradation of organic contaminants, Chem Eng. J. 411 (2021) 128392, https://doi.org/10.1016/j.cej.2020.128392.

[39] M. Sanchez-Polo, J. Lopez-Penalver, G. Prados-Joya, M. A. Ferro-Garcia, J. Rivera-Utrilla, Gamma irradiation of pharmaceutical compounds, nitroimidazoles, as a new alternative for water treatment, Water Res. 43 (2009) 4028–4036, https://doi.org/10.1016/j.watres.2009.05.033.

[40] M. M. Abdel daiem, J. Rivera-Utrilla, R. Ocampo-Perez, M. Sanchez-Polo, J. J. Lopez-Penalver, Treatment of water contaminated with diphenolic acid by gamma radiation in the presence of different compounds, Chem. Eng. J. 219 (2013) 371–379, https://doi.org/10.1016/j.jwpe.2019.100880.

[41] M. El-Desawy, M. A. Zayed, Y. Farrag, Fragmentation pathway of doxazosin drug: thermal analysis, mass spectrometry and DFT calculations and NBO analysis, J. Pharm. Appl. Chem. 3 (2017) 45–51, https://doi.org/10.18576/jpac/030106.

[42] R. Nageswara, D. Nagaraju, A. K. Das, N., Jena, Separation, characterization and quantitation of process-related substances of the anti-hypertensive drug doxazosin mesylate by reversed phase LC with PDA and ESI-MS as detectors, J. Chrom. Sci. 45 (2007) 63–69, https://doi.org/10.1093/chromsci/45.2.63.

[43] W. L. Fitch, C. Khojasteh, I. Aliagas, K. Johnson, Using LC retention times in organic structure determination: drug metabolite identification, Drug Metab. Lett. 12 (2018) 93–100, https://doi.org/10.2174/1872312812666180802093347.

[44] M. R. Clark, L. E. Garcia-Roura, C. R. Clark, Intramolecular hydrogen bonding effects on reversed-phase retention of substituted acetophenones, J. Loq. Chromatogr. 11 (1988) 3213–3221, https://doi.org/10.1080/01483918808076790.

[45] T. S. Alkhuraiji, S. O. B. Boukari, F. S. Alfadhl, Gamma irradiation-induced complete degradation and mineralization of phenol in aqueous solution: Effects of reagent, J. Hazard. Mater. 328 (2017) 29–36, https://doi.org/10.1016/j.jhazmat.2017.01.004.

[46] J. Martini, C. A. Orge, J. L. Faria, M. F. R. Pereira, O. S. G. Soares, Sulfamethoxazole degradation by combination of advanced oxidation processes, J. Environ. Chem. Eng. 6 (2018) 4054–4060, https://doi.org/10.1016/j.jece.2018.05.047.

[47] J. L. Wang, R., Zhuan, Degradation of antibiotics by advanced oxidation processes: An overview, Sci. Total Environ. 701 (2020) 135023, https://doi.org/10.1016/j.scitotenv.2019.135023.

[48] R. Changotra, J. P.,Guin, S. A. Khader, L. Varshney, A. Dhir, Electron beam induced degradation of ofloxacin in aqueous solution: Kinetics, removal mechanism and cytotoxicity assessment, Chem. Eng. J. 365 (2019) 973–984, https://doi.org/10.1016/j.cej.2018.08.156.

[49] K. S. Tay, N. Madehi, Ozonation of ofloxacin in water: By-products, degradation pathway and ecotoxicity assessment; Sci. Total Environ. 520 (2015) 23–31, https://doi.org/10.1016/j.scitotenv.2015.03.033.

[50] L. Zhu, B. Santiago-Schübel, H. Xiao, H. Hollert, S., Kueppers, Electrochemical oxidation of fluoroquinolone antibiotics: Mechanism, residual antibacterial activity and toxicity change. Water Res. 102 (2016) 52–62, https://doi.org/10.1016/j.watres.2016.06.005.

[51] M. S. Yahia, N. Oturan, K. El Kacemi, M. El Karbane, C. T. Aravindakumar, M. A. Oturan, Oxidative degradation study on antimicrobial agent ciprofloxacin by electro-fenton process: Kinetics and oxidation products, Chemosphere 117 (2014) 447–454, https://doi.org/10.1016/j.chemosphere.2014.08.016.

[52] E. Illés, A. Tegze, K. Kovács, G. Sági, Z. Papp, E. Takács, L. Wojnárovits, Hydrogen peroxide formation during radiolysis of aerated aqueous solutions of organic molecules, Rad. Phys. Chem. 134 (2017) 8−13, https://doi.org/10.1016/j.radphyschem.2016.12.023.

[53] X. Chen, J. Wang, Degradation of norfloxacin in aqueous solution by ionizing irradiation: Kinetics, pathway and biological toxicity, Chem. Eng. J. 395 (2020) 125095, https://doi.org/10.1016/j.cej.2020.125095.